Carbohydrate Polymers 204 (2019) 170–181

Contents lists available at ScienceDirect

Carbohydrate Polymers

journal homepage: www.elsevier.com/locate/carbpol

Supramolecular hydrogels of β-cyclodextrin linked to calcium homopoly-L-guluronate for release of coumarins with trypanocidal activity

M. Moncada-Basualto[a,b,*], B. Matsuhiro[a], A. Mansilla[c,d], M. Lapier[e], J.D. Maya[e], C. Olea-Azar[b]

[a] Departamento de Ciencias del Ambiente, Facultad de Química y Biología, Universidad de Santiago de Chile, Av. L. B. O'Higgins 3363, Santiago, Chile
[b] Departamento de Química Inorgánica y Analítica, Facultad de Ciencias Química y Farmacéuticas, Universidad de Chile, Av. Sergio Livingstone 1007, Santiago, Chile
[c] Laboratorio de Macroalgas Antárticas y Subantárticas, Universidad de Magallanes, Av. Bulnes 1465, Punta Arenas, Chile
[d] Instituto de Ecología y Biodiversidad, Chile
[e] Departamento de Farmacología Molecular y Clínica, Facultad de Medicina, Universidad de Chile, Av. Independencia 1107, Santiago, Chile

ARTICLE INFO

Keywords:
Homopoly-L-guluronate
3-Amidocoumarins
Inclusion complex
Trypanosoma cruzi
Supramolecular hydrogel
Sub-Antarctic macroalgae

ABSTRACT

Association constants and thermodynamicsparameters on inclusion of four 3-amido coumarins that present trypanocidal activity, into 6-amino-β-cyclodextrin (1:1 stoichimetry) were determined. In addition, pure homopolymeric-α-L-guluronate fraction prepared by partial hydrolysis of sodium alginate from Sub-Antarctic Kelp *Durvillaea antarctica* was conjugated with 6-amino-β-cyclodextrin (64% yield). To glycoconjugates, 3-amido coumarins were incorporated (73% of encapsulation) and supramolecular hydrogels were prepared by gelation with Ca^{2+} ions.

The trypanocidal activity of the inclusion complexes increased by 10%. Likewise, an increase in diffusion in artificial membrane was observed (13%). It was found that the inclusion complexes increased the variation of the mitochondrial potential of *T. cruzi* (17%).

The lowest release of substituted amidocoumarins (ACS) from supramolecular hydrogels occurred at pH 1.2 whereas the maximum release (34%) was observed at pH 8.0. Encapsulation of lipophilic bioactive compounds in supramolecular hydrogels allows the generation of release systems sensitive to pH with potential application in biomedicine.

1. Introduction

Chagas disease is a pathology caused by the protozoan parasite *Trypanosoma cruzi* (*T. cruzi*) and affects approximately 7 million people worldwide (Nunes, Dones, Morillo, Encina, & Ribeiro, 2013). Despite being endemic in Latin America, the disease has progressed towards North America, Europe and several countries of the Western Pacific. Outside endemic regions, the largest burden occurs in the US, where 300,000 people live with this illness (Ferreira & Andricopulo, 2016; Pérez-Molina & Molina, 2018). Nifurtimox and benznidazole are the only two drugs available for treatment of Chagas disease, but have several drawbacks, such as low efficacy, high toxicity and multiple side effects (Pérez-Molina & Molina, 2018). Therefore, there is a need for new, more effective and safe drugs for the treatment of this disease (Freitas et al., 2009).

It has been described that antioxidant compounds, such as flavonoids, may be used to alleviate adverse effects of infection on animal tissues (Kobo et al., 2014). Also, it has been reported that some coumarins are effective in regression of Chagas disease by inhibiting glyceraldehyde-3-phosphate dehydrogenase enzyme (GAPDH), which is important in the glycolytic pathway of parasites (Figueroa-Guinez et al., 2015; Menezes et al., 2003). The trypanocidal activity of a select series of 3-amidocoumarins ontrypomastigote and epimastigote forms of *T. cruzi* was demonstrated in previous studies; it was found that the possible mechanism of action implies generation of oxidative stress in parasites(Moncada-Basualto et al., 2018).

Despite the potential use of coumarins and their derivatives as trypanocidal agents, their application is limited due to their low solubility in water, which is related to low bioavailability. Application of light would allow increase of trypanocidal activity of bioactive compounds such as coumarins. According to the literature, use of these compounds as photosensitizers, could produce photoreduction of coumarins, generating oxidative stress in protozoan parasites (Reszka, Cruz, & Docampo, 1986; Miranda, Miranda et al., 2017; Miranda, Volpato et al., 2017).

On the other hand,it should be noted that bioactive compounds can

* Corresponding author at: Departamento de Ciencias del Ambiente, Facultad de Química y Biología, Universidad de Santiago de Chile, Av. L. B. O'Higgins 3363, Santiago, Chile.
E-mail address: mauricio.moncada@usach.cl (M. Moncada-Basualto).

https://doi.org/10.1016/j.carbpol.2018.10.010
Received 1 August 2018; Received in revised form 11 September 2018; Accepted 4 October 2018
Available online 09 October 2018
0144-8617/

be modified by metabolism factors such as pH changes, temperature changes and enzymatic degradation. One strategy that allows to increase solubility and preserve properties of bioactive compounds in physiological media is the formation of inclusion complexes with cyclodextrins. Chen, Liu, Dong, and Sun (2013), studied formation of inclusion complexes of simple coumarin derivatives with 2-hydroxypropyl-β-CD (HP-β-CD) in water and phosphate buffered saline (pH 7), finding an increase in the solubility of coumarin derivatives as a function of concentration of HP-β-CD in both media.

Regarding the trypanocidal activity of inclusion complexes with cyclodextrins (CD), it has been described that benznidazole complexes with β-CD increase solubility and bioavailability of drug, which presented lower toxicity than free benznidazole in human cells (De Melo et al., 2013, 2016; Leonardi, Bombardiere, & Salomon, 2013; Soares-Sobrinho et al., 2012). Therefore, it is important to study the effect of inclusion of substituted 3-amidocumarins with trypanocidal activity in β-CD.

β-CD and its derivatives are compounds most used for formation of inclusion complexes. However, due to low aqueous solubility, β-CDs have been conjugated to several polymers in order to modify physicochemical properties, improve biocompatibility and improve capacity of drug administration (Auzély-Velty, 2011). Crosslinking of polymer networks conjugated with β-CDs allows the generation of hydrogels, which are used as controlled release systems of drugs (Hoffman, 2002).

Hydrogels are three-dimensional polymeric materials formed by water-soluble polymers which, when crosslinked, become insoluble. Main characteristic of these matrices is the ability to absorb large amounts of water or some other polar solvent, increasing several times their mass (Deligkaris, Tadele, Olthuis, & van den Berg, 2010; Peppas, Bures, Leobandung, & Ichikawa, 2000). Use of natural products in the preparation of hydrogels has taken on a relevant role, because these generally confer properties of biodegradability and biocompatibility, fundamental properties increasingly required in biopharmaceutical applications (Bhattarai, Gunn, & Zhang, 2010). Alginic acid is commonly used in the preparation of hydrogels, it's a copolymer of D-mannuronic acid and L-guluronic acid, which is synthesized in the cellular wall of brown algae (Phaeophyceae) (Azeem, Batool, Iqbal, & Ikram ul, 2017; Chandía, Matsuhiro, & Vásquez, 2001; Chandía, Matsuhiro, Mejías, & Moenne, 2004; Leal, Matsuhiro, Rossi, & Caruso, 2008; Lee & Mooney, 2012; Li, Chen, Yi, Zhang, & Ye, 2010; Martínez-Gómez, Mansilla, Matsuhiro, Matulewicz, & Troncoso-Valenzuela, 2016; Svanem, Skjak-Braek, Ertesvag, & Valla, 1999) and is found in different proportions, in the form of calcium and magnesium salts

Despite the widespread use of hydrogels as a controlled drug release system, their use is limited. The high-water content, essential for biocompatibility, allows only polar molecules to be effectively incorporated into the aqueous phase of hydrogel and once it is administered to organisms, the release is generally too fast for therapeutic purposes (Dos Santos, Couceiro, Concheiro, Torres-Labandeira, & Alvarez-Lorenzo, 2008; Martínez-Gómez, Guerrero, Matsuhiro, & Pavez, 2017). This fact is explained by the insignificant hydrodynamic impediment to the movement of small hydrophilic molecules, due to low micro viscosity of polymer network (Alvarez-Lorenzo, Gómez-Amoza, Martínez-Pacheco, Souto, & Concheiro, 1999). It has been shown that polymers conjugated with β-CDs amplify the affinity of hydrogels towards apolar molecules (Demir, Kahraman, Bora, Kayaman Apohan, & Ogan, 2008; Mocanu, Mihai, LeCerf, Picton, & Moscovici, 2009; Wahid, Wang, Zhong, & Chu, 2017; Wu et al., 2017). The affinity of host molecule with β-CD cavity gives hydrogels a unique mechanism to control loading and delivery of drugs, calling them supramolecular hydrogels.

Izawa et al. (2013) prepared hydrogels by interact with calcium ion and sodium alginate conjugated with 6-aminoethylamino-β-CD, using ondansetron, as a model drug. They found that supramolecular hydrogels responded to mechanical stimuli for drug release. It was also found that the amount of encapsulated drug in the supramolecular hydrogel was eight times higher than a hydrogel without conjugation with β-CD derivative. Despite the wide applicability of hydrogels in administration of drugs, there is little information about generation of supramolecular hydrogels containing bioactive molecules.

Durvillaea antarctica (Chamisso) Hariot in Chile is a large kelp commonly found on exposed rocky shores of Chilean coastline. It is endemic to Southern Hemisphere (Mansilla, Avila, & Cáceres, 2017). In this study we use samples of *D. antarctica* from Magellan ecoregion (51–56 °S) close to the Antarctic continent and considered one of the last pristine places in the world and where it is currently not commercialized. *D. antarctica* is a species with present reproductive individuals throughout the year, similar to populations of this species described for other sub-Antarctic latitude. It is possible that there could be a cryptic species in the region, presenting morphological and reproductive variability that did not agree well with the circumscription of species (Méndez et al., 2017).

In this work, a glycoconjugate was prepared by amidation of homopoly-L-guluronic acid block obtained from *D. antarctica* sodium alginate with mono-6-amino-β-CD. In addition, trypanocidal activity and effect in mitochondrial membrane potential (ΔΨm) of inclusion complexes of four 3-amidocoumarins in β-CD, and liberation of 3-amidocoumarins encapsulated into the glycoconjugates that formed supramolecular hydrogels by interaction of Ca^{2+} ions were studied.

2. Experimental

2.1. Materials and methods

Reagent grade chemicals were purchased from Sigma-Aldrich Chemical Co. (St. Louis, MO, USA) and solvents were purchased from Merck (Darmstadt, Germany). FT-IR spectra in KBr pellets (10% w/w) were recorded in the 4000–400 cm^{-1} region using a Bruker IFS 66*v* instrument (Billerica, MA, USA), second derivative spectra were acquired using the OPUS/IR v.1.44 software incorporated into the hardware of instrument (Leal et al., 2008), samples were previously dried for 8 h *in vacuo* at 56 °C. ^{1}H (400.13 MHz) and ^{13}C (100.62 MHz) NMR spectra were recorded in D_2O, after isotopic exchange (3 x 0.75 mL) at room temperature on a Bruker Avance DRX 400 spectrometer (Bruker, Coventry, UK) using the sodium salt of 3-(trimethylsilyl)-1-propionic-2,2,3,3-d_4 acid as internal reference.Two-dimensional experiments were performed using a pulse field gradient incorporated into an NMR pulse sequence. The number of scans in each experiment was dependent on sample concentration. Molecular weight of alginate and their fractions were determined by the reducing end method (Cáceres, Carlucci, Damonte, Matsuhiro, & Zúñiga, 2000). Optical rotations were measured with a Perkin-Elmer 241 polarimeter (PerkinElmer, Waltham, Massachusetts, USA).

Durvillaea antarctica (Durvillaceae, Phaeophyceae, Ochrophyta*)* was collected in El Aguila Bay (53° 28′ S, 70° 47′ W) Punta Arenas and Seno Otway (52° 53′ S, 71° 07′ O), San Isidro,Magellan ecoregion,Chile.

Mono-6-amino-6-deoxy-β-cyclodextrin (6-NH_2-β-CD) was synthesized according to Tang and Ng (2008), precursor β-cyclodextrin was obtained from AK Scientific Inc (Palo Alto, CA, USA). Elemental analysis of glycoconjugates was performed in Fisons EA1108 equipment at Facultad de Química, Universidad de Concepción, Concepción, Chile.

Synthesis of 3-acrylamidecoumarin (1), 3-acrylamide-4-hydroxycoumarin (2), N-thiophene-3-carboxamidecoumarin (3) and 4-hydroxy-*N*-thiophene-3-carboxamidecoumarin (4) was previously described by Moncada-Basualto et al. (2018). Epimastigote Dm28c strain of *T. cruzi* and RAW 264.7 cells were obtained from an in-house collection (Molecular and Clinical Pharmacology Program, Facultad de Medicina, Universidad de Chile, Santiago, Chile).

2.2. Extraction and purification of alginate

A sample of dry blades of *D. antarctica* was treated according to the

methodology described by Martínez-Gómez et al. (2016). Defatted blades were extracted with 1800 mL of 3% Na_2CO_3 aqueous solution at 95 °C for 4 h. The mixture was centrifuged at 3000 × *g* (Kubota KS-300P, Tokyo, Japan) and the supernatant was dialyzed against distilled water using Spectra/Por membrane ((MWCO 3500) (Spectrum Laboratories, Rancho Dominguez, CA, USA) for two days, concentrated *in vacuo*, poured over three times of its volume in ethanol and centrifuged. The pellet was dissolved in hot water, and freeze-dried (Christ Alpha 1–2 freeze dryer, Osterode am Harz, Germany). The extract was purified, by sequential precipitation in HCl and $CaCl_2$ solutions as previously described (Venegas, Matsuhiro, & Edding, 1993).

2.3. Fractionation of alginate

Purified alkaline extract sample was partially hydrolyzed with HCl according to Haug, Larsen, and Smidsrød (1974). Briefly, sample was heated with 0.3 M HCl at 100 °C for 0.5 h under nitrogen atmosphere, cooled and centrifuged. The supernatant was dialyzed against distilled water, concentrated and poured into five volumes of ethanol, affording fraction 1. The pellet was stirred with 0.3 M HCl at 100 °C for 2 h; neutralized and precipitated with 1 M HCl at pH 2.85. By centrifugation, a soluble fraction (Fraction 2) and a precipitate (Fraction 3) were obtained. Fractions were purified by dialysis, precipitated into ethanol, dissolved in the minimum volume of water and freeze-dried.

2.4. Inclusion complex

Formation of inclusion complexes of 3-amidocumarins with 6-NH_2-β-CD was carried out according to Folch-Cano et al. (2011). Briefly, complexes were prepared by mixing a methanolic solution of the 3-amidocoumarins with NH_2-CD solution in phosphate buffer (pH 7.4), in 1:3 molar ratio. Concentration of methanol in the mixture did not exceed 10% by volume.

Determination of association constant was carried out through fluorescence intensity measurements of 3-amidocoumarins, and emission spectra were recorded between 300–550 nm at a fixed excitation wavelength between 280–330 nm. Association constant was obtained by linear equation of Benesi-Hildebrand (Ackermann, 1987; Tablet, Matei, & Hillebrand, 2012).

$$1/((F - F_0)) = 1/(K_C\ (F_\infty - F_0)\ [\beta CDs]_0) + 1/((F_\infty - F_0)) \quad (1)$$

F_∞ is the fluorescence of 3-amidocoumarin included in NH_2-CD and F_0represents fluorescence of free 3-amidocoumarin.

Thermodynamics parameters of inclusion were obtained through Van't Hoff equation (Acuña-Rougier & Olea-Azar, 2013).

$$\text{Ln } K_C = \Delta H^\circ/(R(T + 273.15\ K/^\circ C)) + (\Delta S^\circ)/R \quad (2)$$

where R is the universal gas constant ($8.314\ J\ K^{-1}\ mol^{-1}$) and T is temperature in Celsius degree.

2.5. Evaluation of the cytotoxic and trypanocidal activity

2.5.1. Cytotoxicity assay

Effect of inclusion complexes on RAW 264.7 cells, cultured in RPMI 1640 medium and supplemented at 5% with fetal bovine serum, was evaluated with 3[4,5-dimethylthiazol-2-yl]-2,5-diphenyltetrazolium bromide dye (MTT) assay as a viability test (Mosmann, 1983). An aqueous solution of inclusion complex was added to culture medium at concentrations of $IC_{50}$of included compounds previously determined by Moncada-Basualto et al. (2018). Plates were further incubated at 37 °C overnight, and optical density of wells was determined using a microplate reader (Asys Expert Plus©, AsysHitach, Austria) at 570 nm. All experiments were performed at least three times and data reported as means and their standard deviations from triplicate.

IC_{50}concentration of ACS in inclusion complexes was determined by Lucas-Abellán equation (Lucas-Abellan, Fortea, Gabaldon, & Nunez-Delicado, 2008). All assays were performed in darkness.

$$[ACS]_F = (-([CD]_0K_C\text{-}[ACS]_0\ K_C + 1) + \sqrt{([CD]_0\ K_C\text{-}[ACS]_0\ K_C + 1)^2 + 4K_C\ [ACS]_0}))/2K_C \quad (3)$$

where $[ACS]_F$: free 3-amidocoumarin

2.5.2. Epimastigote stage viability study

Trypanocidal activity was evaluated against *Trypanosoma cruzi* epimastigote stage (clone Dm28c). It was measured through MTT assay, according to the methodology described by Vieites et al. (2008). Inclusion complexes added to 3×10^6 parasites/mL in LIT culture medium at 28 °C for 24 h, at IC_{50} of previously determined coumarins by Moncada-Basualto et al., 2018. Likewise, Nifurtimox was added as a positive control. Then, tetrazolium salt was added at a final concentration of 0.5 mg/mL, incubated at 28 °C for 4 h, solubilized with 10% SDS/0.1 mMHCl and incubated overnight. After incubation, number of viable parasites was determined by absorbance at 570 nm in a multiwell plate reader (Asys Expert Plus). Untreated parasites were used as controls (100% of viability).All assays were performed in darkness.

2.5.3. Determination of the effect on mitochondrial membrane potential (ΔΨm) in Dm28c epimastigotes of T. cruzi

Mitochondrial membrane potential (ΔΨm) was determined by incorporation of the fluorescent probe tetramethylrhodamine methyl ester (TMRM) (Genes, Baquero, Echeverri, Maya, & Triana, 2011). Epimastigotes of Dm28c strain (1×10^7 parasites/mL) were seeded in a 96-well plate, compounds and inclusion complexes were added to concentration of IC_{50}. Then, carbonylcyanide-*m*-chlorophenylhydrazone (CCCP, 10 μM) was added, and incubated at 28 °C in humified air and 5% CO_2 for 3 h. Cells were washed with phosphate-buffered saline (pH 7.4) and suspensions were incubated with TMRM (50 nM) for 15 min. Incorporation of probe was determined by fluorescence measurements at an excitation wavelength of 550 nm and emission of 590 nm.All assays were performed in darkness

2.6. Parallel artificial membrane permeability assays (PAMPA)

Determination of permeability in artificial membrane of substituted 3-amidocoumarins was carried out according to the methodology described by Sierpe et al. (2017). Donor plates contained 300 μL of the sample at a concentration of 0.5 mM (solubilized in 30% DMSO:70% phosphate buffer pH 7.4).

Quantification of compounds was carried out by spectrophotometry in a microplate spectrophotometer (Multiskan Spectrum, Thermo Electron Co.). PAMPA assay was performed in triplicate (n = 3) and experiments were carried out at least three times, data reported as means and their standard deviations from triplicate.

2.7. Conjugation of homopoly-L-guluronatewith6-NH2-β-CD

Formation of an amide bond between amino group of 6-NH_2-β-CD and carboxylate group of Fraction 3, obtained in partial hydrolysis of alkaline extract was performed, according to the methodology of Han et al. (2012) and Leal, De Borggraeve, Encinas, Matsuhiro, and Müller (2013). Briefly, aqueous solutions of Fraction 3 and 6-NH_2-β-CD were mixed at room temperature and 1-ethyl- (3-3-dimethylaminopropyl) carbodiimide (EDC) and N-hydroxysuccinimide (NHS) were added. A weight ratio of 1:1 between Fraction 3 and NH_2-CD, and Fraction 3:EDC:NHS molar ratio of 2:2:1 were used with reference to the carboxylate groups,pH was controlled at a value of 3.8–4.0 using 0.1 M HCl. Reaction mixture was maintained at room temperature for 12 h with constant stirring and subsequently, it was treated with a THF-hexane solution (4:1). The aqueous phase was concentrated *in vacuo*,

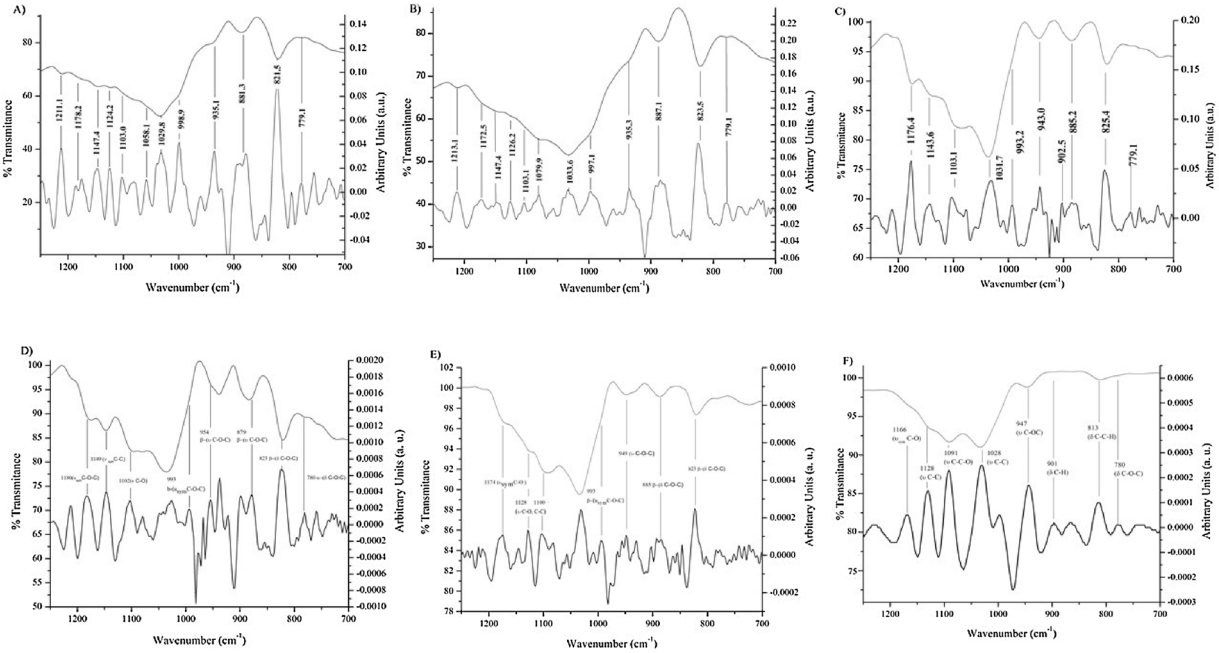

Fig. 1. Normal (above) and second derivative (below) FT-IR spectra of (**A**) milled and dried samples of *D. antarctica* collected inAguila Bay, (**B**) milled and dried samples of *D. antarctica* collected inSeno Otway, (**C**) purified alkaline extract of *D. antarctica*; (**D**) F1, (**E**) F2 and (**F**) F3 fractions obtained by partial acid hydrolysis of the alkaline extract from *D. antarctica*.

dialyzed against distilled water for 48 h and dried by lyophilization.

2.8. Scanning electron microscopy analyses (SEM)

Gold coated hydrogels were analyzed in a NanoSEM NPE 67 equipment (FEI, OR, USA) with an accelerating voltage of 5 kV.

2.9. Swelling ratio determination

Supramolecular hydrogels were generated by adding a solution of glycoconjugate (3.0 mg/mL) to a 0.1 M calcium chloride solution with gentle stirring, and the formed hydrogel was kept in aqueous medium for 2 h. Then, gel was removed, dried with1 Whatman filter (Whatman International, Ltd, Maidstone, England)and left in an oven at 40 °C. Dried hydrogels were added to a solution of H_2O/DMSO in 80/20 ratio and increase in gel mass was determined as a function of time. Monitoring of swelling capacity was carried out for 72 h at room temperature. Swelling ratio were measured by gravimetric method according to Eq. (4).

$$\text{Swelling ratio} = (W_s - W_d)/W_d \quad (4)$$

where W_s and W_d are the weights of swollen and dry supramolecular hydrogels.

Effect of pH and temperature in swelling of supramolecular hydrogels, were studies in three media that emulated different areas of gastrointestinal tract. First medium emulated the stomach under conditions of gastric emptying (pH 1.2) for 2 h and the second and third prepared media emulated areas related to small intestine, duodenum, jejunum and ileum (pH 6.5 and 8.0, respectively).

2.10. In vitro release studies of substituted 3-amidocoumarins

A solution of selected substituted amido coumarin in DMSO (final concentration 6 mM) was added to glycoconjugate solution. The resulting mixture was kept with constant stirring at 37 °C for 24 h.Subsequently, it was added to a 0.1 M solution of calcium chloride in DMSO/H_2O mixture at 80/20 ratio and kept for 2 h. Percentage of encapsulation was determined by ACS difference in calcium chloride solution.

ACS release assays were performed in three solutions containing HCl solution (pH 1.2) and sodium carbonate buffers (pH 6.5 and pH 8.0). ACS release amount was followed for 72 h. Collected aliquots were measured for drug content using a EnSpire® multimode plate reader from PerkinElmer (Hamburg, Germany), using pure substituted 3-amidocoumarin hydrochloride as blank. Equal volume of fresh HCl or carbonate buffer solution was replaced into the release medium to maintain constant volume. UV standard absorbance curve for ACS was established 6–60 μMconcentration range. Percentage of ACS release was determined by Eq. (5):

$$\%\ ACS_{Lib} = ([ACS]_L/[ACS]_T) \times 100 \quad (5)$$

where $[ACS]_L$ and $[ACS]_T$ are the liberated and total concentrations of ACS in the supramolecular hydrogels, respectively.

2.11. Kinetics of hydrogel swelling

Diffusion model of Peppas-Korsmeyer (Kim, La Flamme, & Peppas Nicholas, 2003; Korsmeyer, Gurny, Doelker, Buri, & Peppas, 1983) was applied to data obtained from swelling and release processes of substituted 3-amidocumarin. By means of monoexponential analysis of data, constant k and kinetic coefficient n were determined (Eq. (6)).

$$M_t/M_\infty = kt^n \quad (6)$$

whereas M_t = quantity of absorbed water or released drug at time t, M_∞ = quantity of absorbed water or released drug at equilibrium.

Constant n is diffusional parameter, dependent on matrix geometry and physical transport mechanism of solute (water uptake or drug release). Parameter k incorporates polymeric characteristics of the system. These constants are characteristics of the solvent-polymer system.

2.12. Statistical analysis

Statistical analysis was performed using Graph Pad Prism 4.03 (GraphPad Software. San Diego. California USA). Data are expressed as

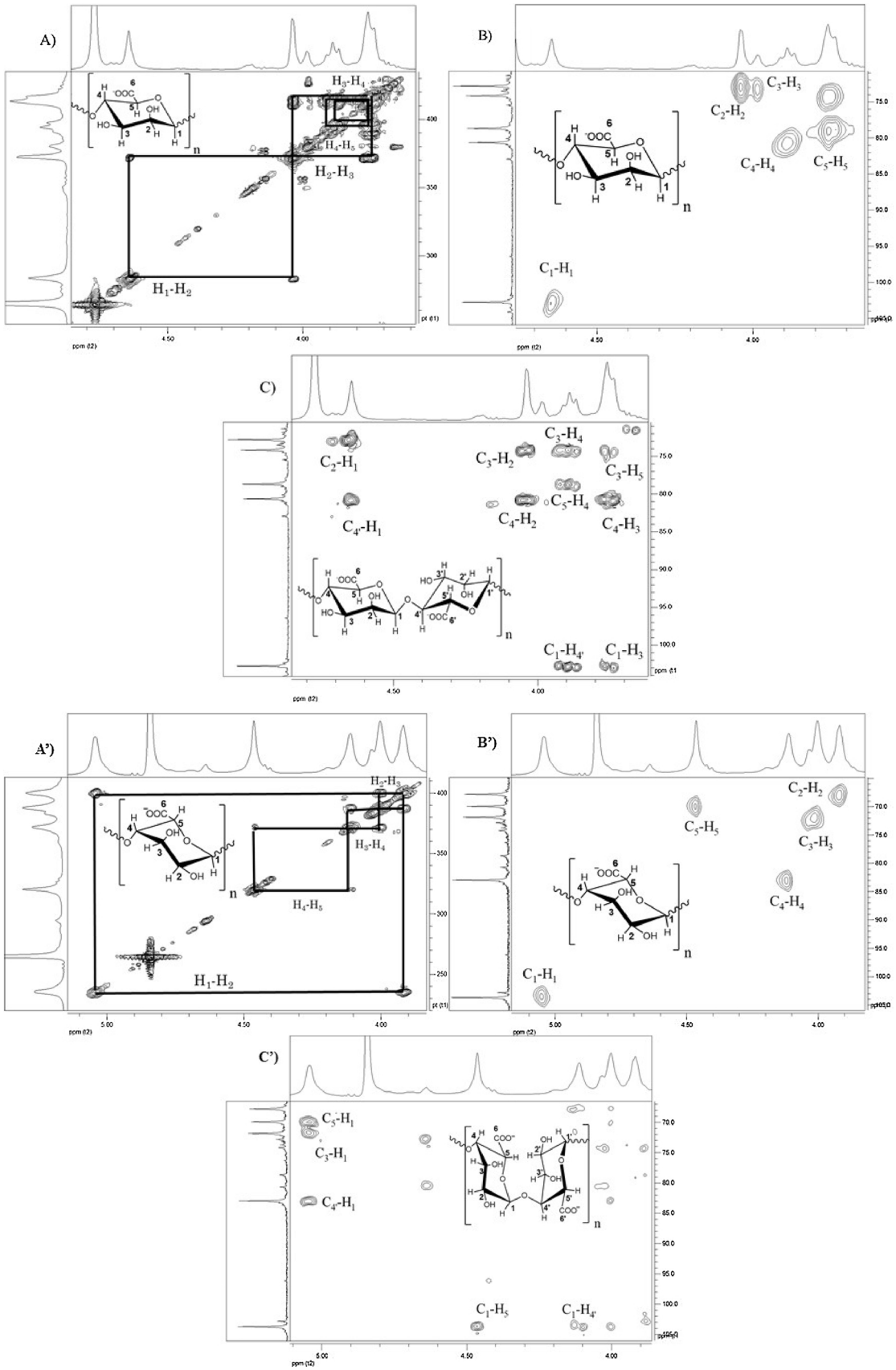

Fig. 2. 2D NMR spectra (**A**)^{1}H/^{1}H COSY, (**B**)^{13}C/^{1}H HSQC, and (**C**)^{13}C/^{1}H HMBC 2D NMR spectra of F2 fraction prepared by partial acid hydrolysis of alkaline extract from *D. antarctica*; (**A'**) COSY ^{1}H/^{1}H, (**B'**) HSQC ^{13}C/^{1}H and (**C'**) HMBC ^{13}C/^{1}H of F3 from acid partial hydrolysis of alkaline extract of *D. antarctica*.

mean ± SD of three independent experiments. Statistical analysis was performed using one-way ANOVA with Dunnett post-test. Data are considered statistically significant when $p < 0.05$

3. Results and discussion

3.1. Extraction and characterization of alginate and block fractions

Fig. 1 presents FT-IR spectra of dried and milled *Durvillaea antarctica* samples collected in two different locations of subantarctic Magellan region. It can be seen that second derivative spectra show more resolved bands and aid to assign characteristic vibrations. Spectra in the region 1300–700 cm^{-1} of both samples are very similar and show characteristic bands of sodium alginate, while second-derivative spectra allowed assigning three characteristic bands of β-mannopyranurosyl residues (938.1, 881.3 and 821.5 cm^{-1}) and one band of less intensity assignable to residues of α-guluronic acid (779 cm^{-1}). These results indicate that alginate from both samples of *D. antarctica* is highly enriched in mannuronic acid. Based on these results, it was decided to work with *D. antarctica* seaweed collected in Aguila Bay.

Seaweed sample was treated with n-hexane, followed by ethanol-formaldehyde mixture in order to eliminate fats and phenols and then, extracted with 3% sodium carbonate. After purification step, 19.4% sodium alginate was obtained. which was lower than that described by Kelly and Brown (2000), for *D. antarctica* (40% of yield), collected on New Zealand east coast.

FT-IR spectrum of the purified extract showed characteristic bands of sodium alginate at 3413 cm^{-1} (ν-OH), 1616 cm^{-1} (ν_{Asym} COO-), and 1415 cm^{-1} (ν_{Sym} COO−). Second derivative spectrum (Fig. 1C) presents in the finger print region characteristic signals at 993 cm^{-1} (ν_{Sym} C—O—C, ν C—O of β glycosidic linkage), 943 cm^{-1} (ν C—C), and 825 cm^{-1} (δ C—O—C of β glycosidic linkage) (Cardenas-Jiron, Leal, Matsuhiro, & Osorio-Roman, 2011; Leal et al., 2008). Spectra are similar to those of milled algal samples and clearly corroborate major presence of β-mannuronic acid in the alkaline extract (Assignment of FT-IR vibration bands in Supplementary material). By integration of anomeric protons in ^1H NMR spectrum in D_2O (figure not shown) a M/G ratio of 2.0 was found. This M/G ratio confirms preliminary results found by FT-IR spectra of *D. antarctic* a alga and alkaline extract, showing that sodium alginate of *D. antarctica* is mostly composed of β-mannuronic acid units.

Sodium alginate from *Durvillaea antarctica* presents a molecular weight of 98,000 g/mol, higher than that found by Martínez-Gómez et al. (2016) for sodium alginates extracted from Antarctic brown algae *Ascoseira mirabilis* (13,000 g/mol) and *Desmarestia ligulata* (48,500 g/mol), but lower than value reported for sodium alginate from Subantarctic *Durvillaea* sp. (278,100 g/mol). It has been described that molecular weight of alginates is influenced by climatic factors of the area where it grows. In general, large algae contain alginate of higher molecular weight, than those of smaller size.

Partial acid hydrolysis of purified alkaline extract afforded three fractions. According to Haug, Larsen, and Smidsrød (1974), fraction 1 (F1) obtained in the first hydrolysis step was enriched in heteropolymeric blocks (MG), the soluble fraction 2 at pH 2.85 (F2) was composed mainly of polymannuronic acid (MM) and fraction 3 insoluble at pH 2.85 (F3) was enriched in polyguluronic acid (GG). F2 fraction is the major fraction obtained by partial hydrolysis of alkaline extract (60% yield) confirms information obtained by spectroscopic methods; for fractions F1 and F3 a yield of 22% and 18% was obtained, respectively. Molecular weights of fractions F1, F2 and F3were 31,000 g/mol, 37,000 g/mol and 29,000 g/mol, which were greater than those obtained by Martínez-Gómez et al. (2016), for fractions of sodium alginate from brown algae of Chilean Antarcticregion.

Normal and second derivative FT-IR spectra of the three fractions are shown in Fig. 1. Fig. 1D depicts normal and second derivative spectra of F1 fraction in finger print region showing assignments of major signals that indicates the presence of heteropolymeric block (MG) (Cardenas-Jiron et al., 2011). Spectra of F2 fraction (Fig. 1E) depicts characteristic bands of poly-β-mannuronic acid (MM) block fraction, no signals assigned to guluronic acid residues are shown, which indicate the presence of homopoly-β-mannuronate block fraction. It is noteworthy that FT-IR spectra (Fig. 1F) of fraction F3 only presents characteristic bands of homopoly-α-guluronate block fraction (GG), no bands assigned to β-mannuronate residues are shown (Cardenas-Jiron et al., 2011; Leal et al., 2008; Matsuhiro, Leal, & Mansilla, 2012; Matsuhiro, Martínez-Gómez, & Mansilla, 2015). Further assignment of vibrational bands in FT-IR spectra appears as Table in Supplementary material. These spectra are similar to those previously published for fractions obtained by acid hydrolysis of sodium alginates from brown algae collected in different areas of Chilean coast (Chandía et al., 2001; Chandía et al., 2004; Leal et al., 2008; Martínez-Gómez et al., 2016; Matsuhiro, Torres, & Guerrero, 2007).

Results found by FT-IR spectroscopy were confirmed by 2D NMR spectroscopy. Fig. 2A depicts correlations of neighboring protons in 2D $^1H/^1H$ COSY NMR spectrum that allow to assign chemical shifts of protons of β-mannuronate residues (Leal et al., 2008; Martínez-Gómez et al., 2016).$^{13}C/^1H$ HSQC spectrum of fraction F2 (Fig. 2B) shows in ordinate axis 1D ^{13}CNMR spectrum of F2; it can be seen 5 mains signals (carbonyl carbon of carboxylate group appeared at 177.71 ppm) that well correlate with already assigned protons indicating the presence of MM homopolymeric blocks (Leal et al., 2008; Martínez-Gómez et al., 2016; Martínez-Gómez, Guerrero, Matsuhiro, & Pavez, 2018).$^{13}C/^1H$ HMBC NMR spectrum (Fig. 2C) presents correlations corresponding to $C_1/H4'$ and $C4'/H_1$ that are related to the presence of β 1→4 glycosidic linkage in fraction F2.

Fig. 2A' depicts $^1H/^1H$ correlations of five protons in COSY spectrum of F3 fraction, where it is shown a signal at 5.05 ppm characteristic of anomeric protons of α-glycosidi cbonds. Fig. 2B' presents$^{13}C/^1H$ correlations in HSQC spectrum, where signal at 103.59 ppm corresponding to anomeric carbon is shown on the axis of ordinates, that allowed establishing that F3 fraction is mainly constituted by GG homopolymeric blocks. Fig. 2C' shows$^{13}C/^1H$ HMBC spectrum with correlations between C_1/H_4' and C_4'/H_1. indicating the presence of α (1→4) glycosidic bond. Table 1 presents ^1H and ^{13}C NMR chemical shifts of F2 and F3 fractions, values are very similar to those published by Martínez-Gómez et al. (2016), for homopolymeric fractions of sodium β-D-mannuronate and α-L-sodium guluronate.

Absolute configuration of constituent monomers was determined by specificoptical rotation of homopolymeric fractions. High negative values of $[\alpha]_D = -103.5°$ (c,0.8, water) for sodium homopolymanopyranuronate (F2 fraction) and $[\alpha]_D = -109.8°$ (c,0.8, water) for sodium homopolygulopyranuronate (F3 fraction) were determined. These values are similar to those published for sodium homopoly-D-manuronate and homopoly-L-guluronate obtained by acid hydrolysis of sodium alginate and allow to establish that the absolute configuration of mannuronic acid residues is D and absolute configuration of guluronic acid is L in the respective homopolymeric blocks (Martínez-Gómez et al., 2016).

Table 1
Chemical shifts assignments in ^1H and ^{13}C NMR spectra of sodium salts of homopolymannuronic acid (F2), and homopolyguluronic acid (F3).

	δ (ppm)					
	H_1/C_1	H_2/C_2	H_3/C_3	H_4/C_4	H_5/C_5	C_6
F2	4.67/102.87	4.05/72.82	3.78/74.21	3.90/80.83	3.75/78.92	177.71
F3	5.05/103.59	3.93/67.69	4.01/71.78	4.10/82.89	4.45/69.91	178.28

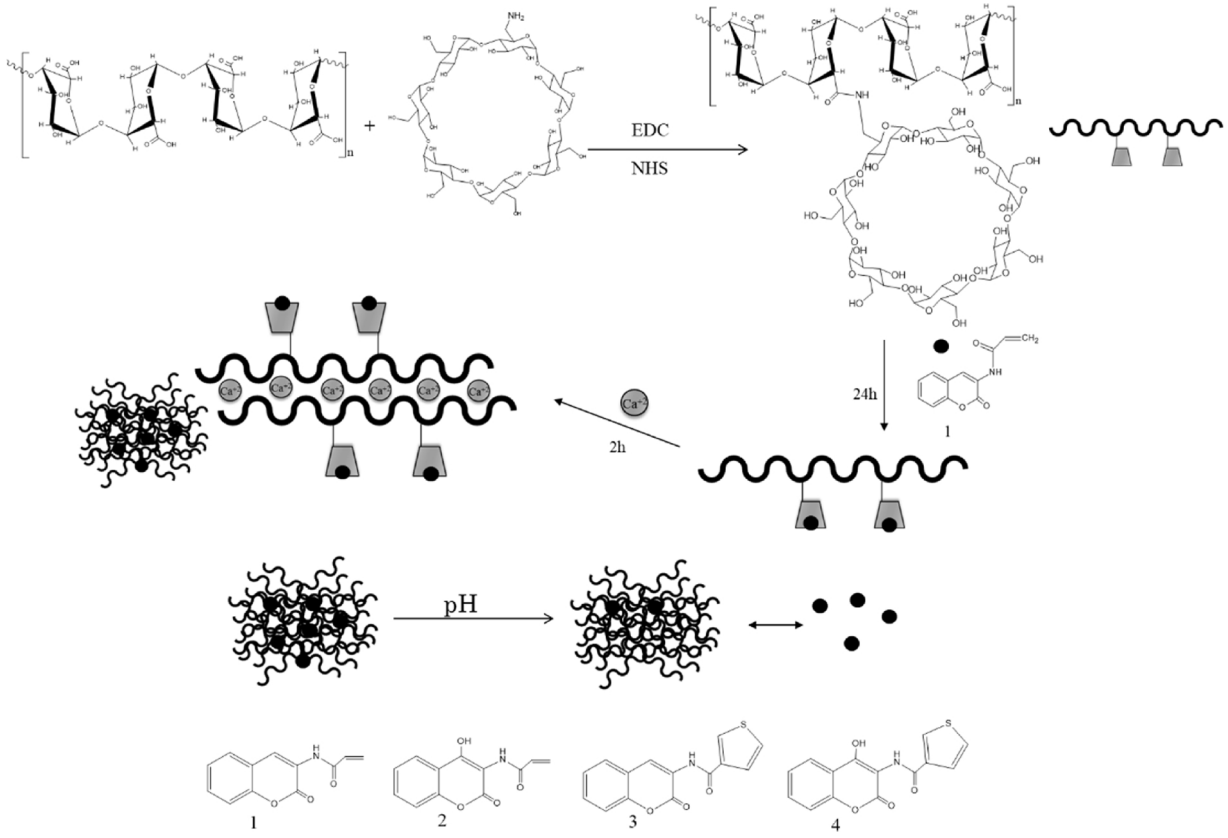

Scheme 1. Schematic representation of the synthesis of GG block glycoconjugate with 6-NH_2-β-CD, formation of supramolecular hydrogels and release of 3-acrylamidecoumarin (**1**), 3-acrylamide-4-hydroxycoumarin (**2**), *N*-thiophene-3-carboxamidecoumarin (**3**) and 4-hydroxy-*N*-thiophene-3-carboxamidecoumarin (**4**).

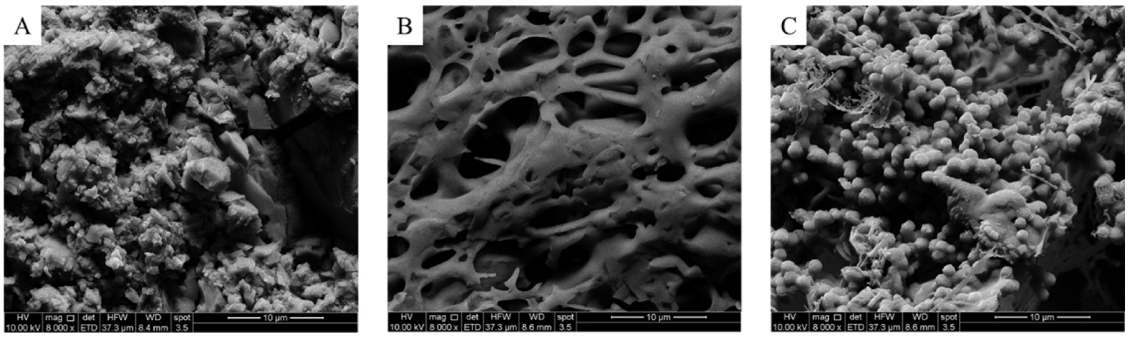

Fig. 3. SEM images of (**A**) 6-NH_2-β-CD, (**B**) homopolymer blocks GG and (**C**) glycoconjugate of GG blocks with 6-NH_2-β-CD.

3.2. Conjugation of sodium homopoly-L-gulopyranuronate with 6-NH2-β-CD

Conjugation was carried out by means of amidation reaction between amino group of mono-6-amino-6-deoxy-β-cyclodextrin and carboxylate group of sodium homopoly-α-L-guluronate block fraction (GG) (Izawa et al., 2013). Conjugation was accomplished with homopoly-L-guluronic acid block fraction taking into consideration its gelling properties in the presence of Ca^{2+} ions. It can be pointed out that tertiary structures of heteropolymeric and homopoly-D-mannuronic acid fractions do not allow formation of gels in presence of calcium cations (Haug et al., 1974; Leal et al., 2013). In addition, it is important to mention the use of pure homopolymeric GG fraction instead of the whole alginate, especially in systems that may have medical applications, in order to get glycoconjugates with known and well defined structure.

Amidation reaction was performed in EDC presence as acylating agent (Scheme 1).

Synthesis was carried out at pH 4.5 to allow reaction of EDC with carboxylate groups present in homopolymer block and the intermediate was stabilized using N-hydroxysuccinimide (NHS) affording a product in 64% yield. FT-IR spectrum of the glycoconjugate (figure not shown), presented bands assignable to stretching of N—H bond (1648 cm^{-1}, amide II) and stretching of the C—N bond (1350 cm^{-1}, amide III); likewise, characteristic bands of GG homopolymer block (780 cm^{-1}, C—O—C). ^1H NMR spectrum of the glycoconjugate (figure no shown) allowed assignment of protons of amide group at low field (7.49 ppm), anomeric proton of GG block (5.01 ppm) and H-6 protons of α-D-glucopyranosil residue bound to homopolymer (2.75 ppm) confirming formation of amide bond. Degree of substitution (DS) determined by ^1H NMR (Chiang & Chu, 2015) and nitrogen content determined by elemental analysis in the synthesized glycoconjugate were 0.23 and 0.97%, respectively. These values are concordant with a ratio of one cyclodextrin units for every 4 units of the GG homopolymer.

Characterization of the glycoconjugate was also performed by SEM. Fig. 3A shows SEM image of 6-NH_2-β-CD in which formation of

irregular structures in crystal forms can be seen, in accordance with those described in literature for β-CD (Louiz, Labiadh, & Abderrahim, 2015; Malaquias et al., 2018). Fig. 3B depicts a homogeneous distribution corresponding to GG homopolymer block. Fig. 3C corresponds to the glycoconjugate showing small spheres with a diameter of 1 μm, approximately, over a regular surface that is attributed to GG blocks.

3.3. Preparation and characterization of inclusion complexes

Selected substituted amido coumarin (1, 2, 3 and 4) inclusion complexes were obtained by adding increasing amounts of 6-NH_2-β-CD, maintaining a fixed concentration of coumarin in aqueous medium, as described by Folch-Cano et al. (2011). Stoichiometry of inclusion complexes was determined by the continuous variation method of Job Plot (Chen et al., 2013; Connors, 1997; Job, 1928). A 1:1 stoichiometry was found for all inclusion complexes. Result is similar to that described for inclusion complexes of hydroxylated coumarin in position 4 and that has an aromatic ring in position 3 of the basic structure of coumarin (Folch-Cano et al., 2011). According to determined stoichiometry, there would be an ACS molecule in the hydrophobic cavity of 6-NH_2-β-CD, which is related to cavity size of β-CD derivative (153 Å) (Pinho, Grootveld, Soares, & Henriques, 2014). In Table 3 values of association constants for ACS complexes with 6-NH_2-β-CD determined by Benesi & Hildebrand equation (Benesi & Hildebrand, 1949) are presented. It should be noted that formation of inclusion complexes and determination of association constants of coumarins with 6-NH_2-β-CD has not been described in literature. Values of association constants obtained are like those found for other coumarins in β-cyclodextrin and hydroxypropyl-β-cyclodextrin (HP-β-cyclodextrin). Hoshiyama, Kubo, Igarashi, and Sakurai, (2001) described for inclusion complexes of hydroxylated coumarins in position 7 values close to 500 M^{-1}. Likewise, Folch-Cano et al. (2011) found similar values of inclusion constants of the order of 750 M^{-1} for 3-phenyl-4-hydroxycoumarin with HP-β-cyclodextrin and β-cyclodextrin.

Thermodynamic parameters: enthalpy (ΔH), entropy (ΔS) and energy of Gibbs (ΔG) of association were determined through association constants at different temperatures obtained by Benesi-Hildebrand equation. ACS present negative values of Gibbs energy (Table 3), which indicate spontaneous formation of inclusion complexes. For complexes that contain coumarin withacroyl group in its structure (ACS 1 and 2), positive values of entropy and enthalpy were obtained, corroborating that the inclusion is driven entropically. This is attributed to loss of degrees of freedom of coumarin and 6-NH_2-β-CD derivative; as well as increase in the entropy of system due to release of highly energetic water molecules from hydrophobic cavity interior. Furthermore, negative entropy values are associated with hydrophobic interactions that restructure water molecules around apolar solutes, where the latter are complexed incyclodextrin cavity, with the aim of exposing smallest possible area to water molecules (Morais, Lemes Silva, Denadai, Fedoce Lopes, & De Sousa, 2017). Positive enthalpy values obtained are result of several factors, among them endothermic contribution due to interruption of hydrogen bonds between water molecules in the cavity and endothermic dehydration of hydrophobic host molecule (Castronuovo, Niccoli, & Varriale, 2007; Rekharsky et al., 1997).

On the other hand, inclusion complexes formed with ACS containing thiophene group (3 and 4) in their structure presented negative values of enthalpy (Table 2), which indicate an exothermic inclusion process that would be mainly controlled by Van der Waals interactions between the host and the cavity of the cyclodextrin (Yang, Liu, Mu, & Guo, 2001). These interactions are constituted by i) dipole-dipole interactions, consisting of interactions between permanent dipoles, ii) induced dipole-dipole, consisting of a permanent dipole that induces a dipole in another molecule and iii) dispersion, which are caused by synchronization of electronic movement between two molecules, resulting in momentary dipoles that are oriented to cause their attraction. Given the polarizability of both molecules (host and guest) these interactions can explain negative enthalpy values (Roy, Saha, & Roy, 2016). Likewise, formation of links by hydrogen bonds between guest and hydroxyl groups of the host must be considered. It is worth mentioning that trends of values of thermodynamic parameters determined in this work are similar to those obtained by Folch-Cano et al. (2011), for inclusion of 3-phenyl-4-hydroxy-7-methoxycoumarin in dimethyl-β-cyclodextrin.

3.4. Biological activities

3.4.1. Cytotoxicity and trypanocidal activity

Trypanocidal activity of inclusion complexes on epimastigotes *Dm28c* was determined at IC_{50} concentration by Eq. (3). Cell viability of inclusion complexes on murine and epimastigote *Dm28c* cells of *T. cruzi* was compared with uncomplexed ACS (Table 3). An increase in trypanocidal activity of non-hydroxylated complex ACS (1 and 3) was observed, which can be related to higher solubility of compounds. It should be noted that 6-NH_2-β-CD did not present trypanocidal or cytotoxic activityin the concentration range used. In relation to cytotoxic activity on murine cells. no significant variation in the toxicity of complexes was observed in relation to free coumarin.

About cytotoxic activity on murine cells, no significant variation in toxicity of complexes was observed in relation to free coumarin. On the other hand, inclusion complexes of 2 and 4 hydroxylated amido coumarins did not show variation in trypanocidal activity in relation to free coumarin. These results are not related to what was previously described for non-hydroxylated ACS complex where an increase in trypanocidal activity was observed, possibly related to increase in bioavailability of these compounds.

Based on above results, parallel permeability in artificial membrane (PAMPA) of complexes and free ACS was determined. Free 1 and 3 ACS showed less than 50% diffusion through artificial membrane. On the other hand, hydroxylated ACS presented high percentages of association to the membrane, which indicates that they do not present passive diffusion in this model membrane. This could explain the differences described above intrypanocidal activity of hydroxylated and non-hydroxylated ACS in epimastigote form of *T. cruzi*.

In Table 3 an increase in the permeability of ACS included in 6-NH_2-β-CD in relation to that determined for free ACS is shown. Greatest variations of permeability in artificial membrane were obtained for complexes of non-hydroxylated ACS.

There are several mechanisms that may explain the fact that cyclodextrin inclusion complexes with adequate association constants can improve absorption and bioavailability of complexed compounds (Réti-Nagy et al., 2015). First mechanism is based on the effect of increasing solubility of coumarin to be included within cyclodextrin cavity. In this way, host molecule can be transported through layers of water surrounding the cell, directly to biological membrane with help of cyclodextrin. Cyclodextrins can increase drug transport only if resistance of water layer on donor side is equal to or greater than resistance of membrane barrier. According to this mechanism, complexed compound is transported to membrane, where the complex dissociates and free molecule penetrates through membrane (Kurkov & Loftsson, 2013; Ren, Gao, Cao, & Jia, 2015). The second action is based on effect of cyclodextrinsin intestinal epithelium; it has been found that lipophilic cyclodextrins (*e.g.*, methyl-β-cyclodextrin) are capable of decreasing barrier function increasing the transport of molecules through biological membranes (*e.g.*, the nasal mucous membrane). However, excess amount of hydrophilic cyclodextrin can decrease penetration of drugs (Loftsson, Vogensen, Brewster, & Konráosdóttir, 2007). Besides effects mentioned above, inhibition of the active transporters in membrane can be important. Many active transporter proteins such as P-glycoprotein can decrease the absorption of substrates by pumping from membrane to outside thereof (Fenyvesi et al., 2014). A mechanism involving endocytosis of inclusion complexes with cyclodextrin has also been described. These molecules are unable to penetrate cell membrane by diffusion due to their molecular size and high hydrophilic character,

Table 2
Association constants at different temperatures and thermodynamic parameters of the inclusion complexes of ACS in 6-NH_2-β-CD.

ACS	Temperature (°C)	Associationconstant (mol^{-1} L)	Enthalpy (kJ mol^{-1})	Entropy (J K^{-1} mol^{-1})	Gibbs energy (kJ mol^{-1})[a]
1	25	473 ± 12	19.35 ± 1.89	116.48 ± 6.25	−15.36 ± 0.03
	30	593 ± 10			
	37	669 ± 15			
	40	698 ± 9.1			
2	25	412 ± 8.7	21.95 ± 2.38	123.93 ± 7.75	−14.98 ± 0.07
	30	504 ± 12			
	37	609 ± 11			
	40	627 ± 10			
3	25	639 ± 13	−11.96 ± 0.89	13.60 ± 3.13	−16.00 ± 0.04
	30	584 ± 8.7			
	37	532 ± 21			
	40	504 ± 15			
4	25	651 ± 9.7	−16.16 ± 0.24	−0.25 ± 0.19	−16.09 ± 0.05
	30	609 ± 15			
	37	512 ± 12			
	40	481 ± 9.5			

[a] Parameter determined at 25 °C.

but the cells can incorporate inclusion complexes of cyclodextrins by endocytosis (Fenyvesi et al., 2011; Yang, Li, Sun, & Zhang, 2018). This mechanism has been demonstrated by the incorporation of fluorescent derivatives of β-cyclodextrin into the cytoplasm of Caco-2 cells (Réti-Nagy et al., 2015). According to the results obtained in this work, the most probable mechanism would be the first (based on the effect of increasing solubility of coumarin) given the hydrophilicity of 6-NH_2-β-CD.

3.4.2. Mitochondrial membrane potential (ΔΨm)

Parasites of *T. cruzi* have only one mitochondrion, which is fundamental for their survival and regulates processes related to energy balance and modulation of apoptosis (Lecca et al., 2015; Menna-Barreto et al., 2009; Nogueira et al., 2017). This could be the intracellular target of compounds under study. Mitochondrial metabolism was evaluated by varying mitochondrial membrane potential (ΔΨm). Fig. 4 shows percentage of incorporation of TMRM probe indicative of variations in mitochondrial membrane potential. For free ACS, minor effects on membrane potential were observed for CCCP decoupling agent and that found by Muñoz et al. (2016), for series of 3-carboxyamide coumarins. Based on these results, it is postulated that there is an effect on mitochondrial function, which could be associated with generation of oxidative stress in *T. cruzi* parasites, as previously demonstrated by Moncada-Basualto et al. (2018).

Effect of inclusion complexes on ΔΨm in epimastigote form of *T. cruzi* was higher in relation to free ACS (Fig. 4). Greater incorporation was obtained in mitochondrial matrix of fluorescent probe TMRM; these results are related to increase in trypanocidal activity of inclusion complexes and the increase in passive diffusion of ACS confirming that one of intracellular targets is the mitochondrial function of parasite (Muñoz et al., 2016).

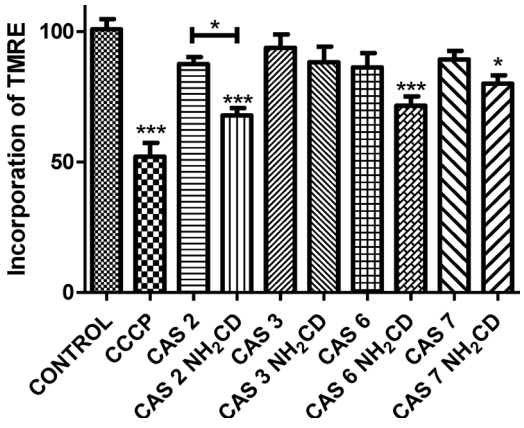

Fig. 4. Percentage of tetramethylrhodamine methyl ester (TMRM) incorporation by mitochondrial membrane potential variation (ΔΨm) in epimastigote form of *T. cruzi* caused by free ACS and complexed with 6-NH_2-β-CD.Significant difference compared to control (one-way ANOVA with Dunnett post-test; *: $p > 0.05$ ***: $p > 0.01$).

3.5. Supramolecular hydrogel

3.5.1. Preparation of supramolecular hydrogels and swelling curves

Formation of supramolecular hydrogels of glycoconjugate of homopoly-L-guluronic block fraction (GG) with 6-NH_2-β-CD was carried out by interaction of free carboxylate group of unconjugated α-L-guluronate residues with Ca^{2+}. Interaction with calcium ions was carried out to generate polymer network responsible for retention of aqueous solutions; thus, achieving the formation of supramolecular hydrogels. It can be mention that according to the literature, glycoconjugation does not significantly modify inclusion capacity of hydrophobic cavity of

Table 3
Percentage of viability of inclusion complexes to concentration of IC_{50} of free ACS on murine cells (RAW 264.7) and parasites of *T. cruzi* Dm28c and association and diffusion in artificial membrane of free ACS and complexed with 6-NH_2-β-CD.

	Inclusion Complexes			ACS		Inclusion Complexes	
	% viability of RAW 264.7 cell	% viability of epimastigote *Dm28c*	ε (M^{-1} cm^{-1})	% association	% diffusion	% association	% diffusion
1	51.08 ± 1.32	41.30 ± 1.12***	17,803 (λ = 320 nm)	52.4 ± 0.3	43.1 ± 0.2	32.1 ± 0.8	66.3 ± 1.1
2	62.11 ± 1.27[a]	51.22 ± 1.31	18910 (λ = 303 nm)	92.3 ± 0.2	–[b]	83.3 ± 0.7	8.6 ± 0.4
3	58.43 ± 1.01[a]	45.03 ± 1.02***	19,770 (λ = 314 nm)	50.3 ± 0.2	47.6 ± 0.3	41.1 ± 1.1	56.2 ± 1.2
4	53.05 ± 1.62*	58.01 ± 1.02[a]	20,100 (λ = 307 nm)	94.6 ± 0.1	–[b]	80.4 ± 0.9	9.1 ± 0.3

[a] 100 μM used of coumarin, Significant difference compared to control (one-way ANOVA with Dunnett post test; *: $p > 0.05$ ***: $p > 0.01$).
[b] Undetermined.

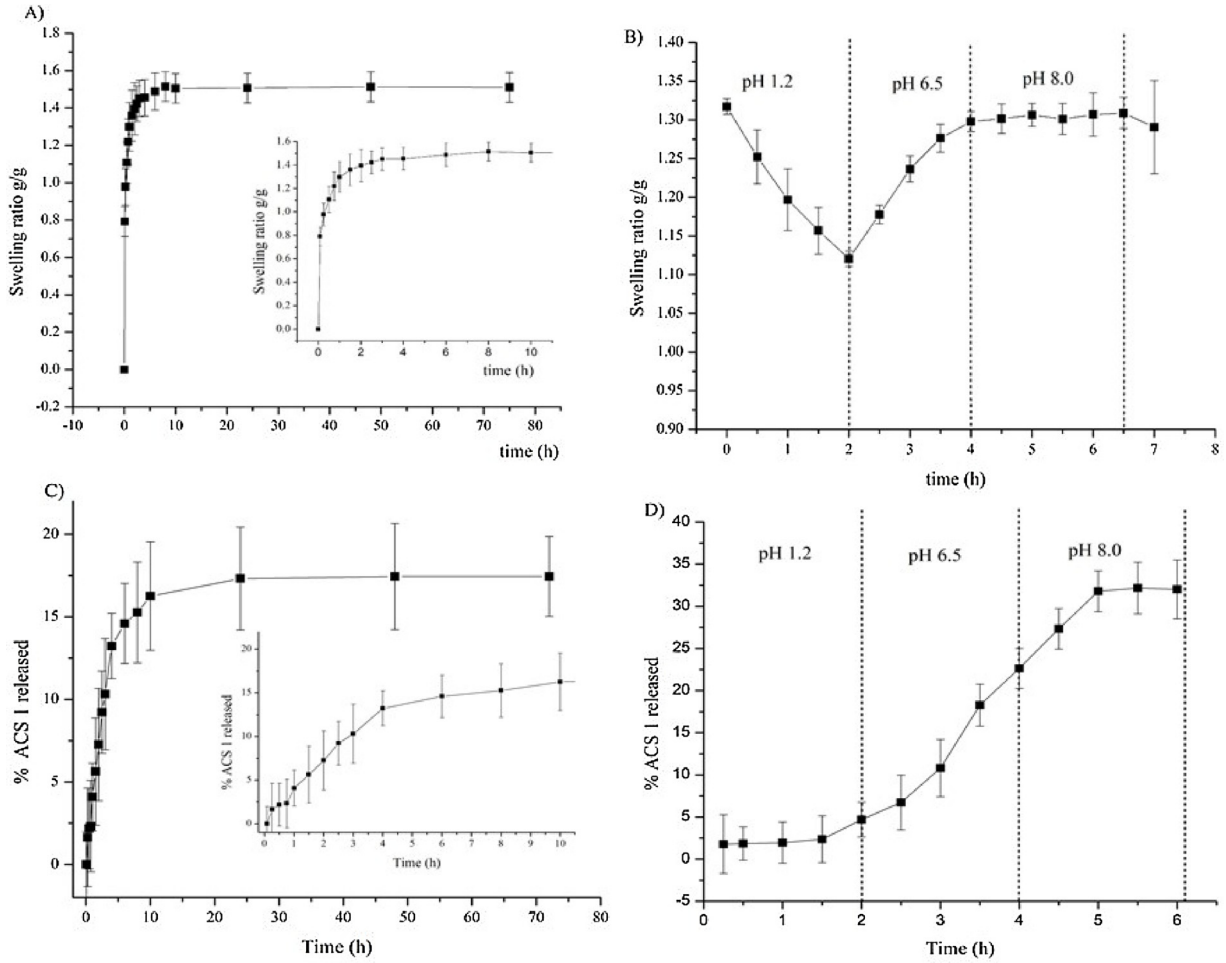

Fig. 5. Swelling curve of supramolecular hydrogel in a mixture of water and DMSO in 80/20relation. (**A**) at room temperature and (**B**) controlled pH; curves of release of ACS 1 to (**C**) at controlled temperature (37 °C) and (**D**) at controlled pH.

cyclodextrins (Concheiro & Alvarez-Lorenzo, 2013; Mocanu et al., 2009).

Fig. 5A shows swelling curve of supramolecular hydrogels. where at 10 h mass was kept constant. After 70 h hydrogels began to crack, losing included water; instability of hydrogels may be associated with mechanisms involved in gelling process. Swelling capacity of supramolecular hydrogel reached 1.5 times its dry weight. This value is lower than that determined for hydrogels of GG blocks and polyvinyl alcohol (Martínez-Gómez et al., 2018).

For studies of the effect of pH on swelling capacities of hydrogels, four media were prepared which emulated four sections of human gastrointestinal tract. In Fig. 5B curve of hydrogel swelling at pH and controlled temperature is presented. It is observed that hydrogels previously swollen have a decrease in the ability to swell at pH 1.2; this can be explained because at this pH carboxylate groups of GG acquired acid form. Swollen capacities are restored at pH 6.5 with low variability and when pH 8 is reached, hydrogels swelling rate is maintained. However, with passage of time, redissolution of gel is observed due to calcium cations exchange by sodium cations (Izawa et al., 2013).

3.5.2. Encapsulation of ACS of supramolecular hydrogels

Percentage of ACS encapsulated in supramolecular hydrogels was determined through determination of ACS in the $CaCl_2$ solution.Supramolecular hydrogels prepared with ACS with acroylgroup 1 and 2 presented percentage of encapsulation of 68.3 ± 0.43% and 71.2 ± 0.27%, respectively; in the case of ACS with thiophene group 3 and 4, 73.5 ± 0.32% and 74.8 ± 0.26% encapsulation were respectively obtained.

3.5.3. Release of ACS from supramolecular hydrogels

ACS release studies were carried out at controlled temperature and pH. ACS was added to a glyconjugate solution, to allow the inclusion in β-CD bound to the polysaccharide, before interaction with Ca^{2+}. Determination of liberated ACS was carried out based on concentration of compound encapsulated. It is observed in Fig. 5C that percentages of release are relatively similar for ACS under study at controlled temperature, achieving a maximum release close to 15% for all ACS under study after 10 h. (Table 4).

Release profiles at controlled pH were similar for all ACS under study (Fig. 5D), where release maxima were reached at pH that emulates ileum. At this pH degradation of polymer matrix was observed which may be related to exchange of Ca^{2+} by Na^{+}, causing redissolution of gel. Release percentages were higher for ACS containingacroyl group in its structure without a marked influence of hydroxyl group on release of bioactive compound.

The diffusion model of Peppas-Korsmeyer (Korsmeyer et al., 1983) was applied in swelling and release studies of selected ACS. Based on the mathematical model of Peppas-Korsmeyer, coefficient n is related to different possible mechanisms associated with transport of a solute inside and outside the matrix (Korsmeyer et al., 1983).

Table 4 shows results obtained for application of the model in curve of swollen at controlled temperature, where mechanism is controlled by diffusion of solvent in polymer matrix.

Parameter n in the release of selected ACS was similar for all

Table 4
Percentage of ACS release at pH and controlled temperature and parameters of Peppas-Korsmeyer diffusional model determined for the process of puffing and releasing selected ACS from supramolecular hydrogels.

Supramolecular hydrogel	% released controlled temp.	% released controlled pH	H_2O/DMSO T = 37 °C			Controlled pH T = 37 °C		
			n	k	R^2	n	k	R^2
Swelling	–	–	0.15	0.44	0.985	–	–	–
ACS 1	17.45 ± 2.42	32.01 ± 3.48	0.86	0.23	0.990	0.88	0.27	0.981
ACS 2	18.49 ± 1.78	34.01 ± 2.12	0.76	0.31	0.982	0.81	0.21	0.992
ACS 3	14.51 ± 2.57	24.42 ± 3.12	0.80	0.27	0.985	0.87	0.25	0.980
ACS 4	15.39 ± 3.12	25.07 ± 2.89	0.81	0.33	0.986	0.83	0.28	0.987

molecules under study, where it is observed that release of bioactive molecules is controlled by erosion of polymeric matrix in accordance with Martínez-Gómez et al. (2017, 2018), which is related to what was observed in area that emulates fraction of ileum (pH 8.0).

4. Conclusions

Inclusion of lipophilic non-hydroxylated coumarins with trypanocidal activity into β-cyclodextrin increases their bioavailability, enabling application of inclusion complexes for the delivery of anti-Chagasic drugs.

Supramolecular hydrogels based on a biopolymer with known structure and specific properties are capable to include and release in a controlled manner lipophilic bioactive compounds constituting a polymeric system with potential biomedical applications.

Acknowledgments

MBM thanks PhD fellowship and Grant N° 21150192 for operational expenses from CONICYT, Chile. The financial support of DICYT, Grant 021641MY (Universidad de Santiago de Chile), COA Grants FONDECYT1150175 and project U-REDES URC-024-16 is gratefully acknowledged. A.M. Grants ICM, P05-002, CONICYT PFB-23.

Appendix A. Supplementary data

Supplementary material related to this article can be found, in the online version, at doi:https://doi.org/10.1016/j.carbpol.2018.10.010.

References

Ackermann, T. (1987). *K. A. Connors: Binding constants—The measurement of molecular complex stability*, *vol. 91*, New York: John Wiley & Sons1398 (12).
Acuña-Rougier, C., & Olea-Azar, C. (2013). Thermodynamic and geometric study of diasteroisomeric complexes formed by racemic flavanones and three cyclodextrins through NMR. *Journal of Inclusion Phenomena and Macrocyclic Chemistry, 75*(1), 119–136.
Alvarez-Lorenzo, C., Gómez-Amoza, J. L., Martínez-Pacheco, R., Souto, C., & Concheiro, A. (1999). Microviscosity of hydroxypropylcellulose gels as a basis for prediction of drug diffusion rates. *International Journal of Pharmaceutics, 180*(1), 91–103.
Auzély-Velty, R. (2011). Self-assembling polysaccharide systems based on cyclodextrin complexation: Synthesis, properties and potential applications in the biomaterials field. *Comptes Rendus Chimie, 14*(2–3), 167–177.
Azeem, M., Batool, F., Iqbal, N., & Ikram ul, H. (2017). *Chapter 1—Algal-based biopolymers A2-Zia, Khalid Mahmood, algae based polymers, blends, and composites.* Elsevier1–31.
Benesi, H. A., & Hildebrand, J. H. (1949). A spectrophotometric investigation of the interaction of iodine with aromatic hydrocarbons. *Journal of the American Chemical Society, 71*(8), 2703–2707.
Bhattarai, N., Gunn, J., & Zhang, M. (2010). Chitosan-based hydrogels for controlled, localized drug delivery. *Advanced Drug Delivery Reviews, 62*(1), 83–99.
Cáceres, P. J., Carlucci, M. A. J., Damonte, E. B., Matsuhiro, B., & Zúñiga, E. A. (2000). Carrageenans from chilean samples of *Stenogramme interrupta* (Phyllophoraceae): Structural analysis and biological activity. *Phytochemistry, 53*(1), 81–86.
Cardenas-Jiron, G., Leal, D., Matsuhiro, B., & Osorio-Roman, I. O. (2011). Vibrational spectroscopy and density functional theory calculations of poly-D-mannuronate and heteropolymeric fractions from sodium alginate. *Journal of Raman Spectroscopy, 42*(4), 870–878.
Castronuovo, G., Niccoli, M., & Varriale, L. (2007). Complexation forces in aqueous solution. Calorimetric studies of the association of 2-hydroxypropyl-β-cyclodextrin with monocarboxylic acids or cycloalkanols. *Tetrahedron, 63*(30), 7047–7052.
Chandía, N. P., Matsuhiro, B., Mejías, E., & Moenne, A. (2004). Alginic acids in *Lessonia vadosa*: Partial hydrolysis and elicitor properties of the polymannuronic acid fraction. *Journal of Applied Phycology, 16*(2), 127–133.
Chandía, N. P., Matsuhiro, B., & Vásquez, A. E. (2001). Alginic acids in *Lessonia trabeculata*: Characterization by formic acid hydrolysis and FT-IR spectroscopy. *Carbohydrate Polymers, 46*(1), 81–87.
Chen, A., Liu, M., Dong, L., & Sun, D. (2013). Study on the effect of solvent on the inclusion interaction of hydroxypropyl-β-cyclodextrin with three kinds of coumarins by phase solubility method. *Fluid Phase Equilibria, 341*(0), 42–47.
Chiang, C.-Y., & Chu, C.-C. (2015). Synthesis of photo responsive hybrid alginate hydrogel with photo-controlled release behavior. *Carbohydrate Polymers, 119*(0), 18–25.
Concheiro, A., & Alvarez-Lorenzo, C. (2013). Chemically cross-linked and grafted cyclodextrin hydrogels: From nanostructures to drug-eluting medical devices. *Advanced Drug Delivery Reviews, 65*(9), 1188–1203.
Connors, K. A. (1997). The stability of cyclodextrin complexes in solution. *Chemical Reviews, 97*(5), 1325–1358.
De Melo, P. N., Barbosa, E. G., de Caland, L. B., Carpegianni, H., Garnero, C., Longhi, M., et al. (2013). Host–guest interactions between benznidazole and beta-cyclodextrin in multicomponent complex systems involving hydrophilic polymers and triethanolamine in aqueous solution. *Journal of Molecular Liquids, 186*(0), 147–156.
De Melo, P. N., Barbosa, E. G., Garnero, C., de Caland, L. B., Fernandes-Pedrosa, M. F., Longhi, M. R., et al. (2016). Interaction pathways of specific co-solvents with hydroxypropyl-β-cyclodextrin inclusion complexes with benznidazole in liquid and solid phase. *Journal of Molecular Liquids, 223*(Suppl. C), 350–359.
Deligkaris, K., Tadele, T. S., Olthuis, W., & van den Berg, A. (2010). Hydrogel-based devices for biomedical applications. *Sensors and Actuators B: Chemical, 147*(2), 765–774.
Demir, S., Kahraman, M. V., Bora, N., Kayaman Apohan, N., & Ogan, A. (2008). Preparation, characterization, and drug release properties of poly(2-hydroxyethyl methacrylate) hydrogels having β-cyclodextrin functionality. *Journal of Applied Polymer Science, 109*(2), 1360–1368.
Dos Santos, J.-F. R., Couceiro, R., Concheiro, A., Torres-Labandeira, J.-J., & Alvarez-Lorenzo, C. (2008). Poly(hydroxyethyl methacrylate-co-methacrylated-β-cyclodextrin) hydrogels: Synthesis, cytocompatibility, mechanical properties and drug loading/release properties. *Acta Biomaterialia, 4*(3), 745–755.
Fenyvesi, F., Réti-Nagy, K., Bacsó, Z., Gutay-Tóth, Z., Malanga, M., Fenyvesi, É., et al. (2014). Fluorescently labeled methyl-beta-cyclodextrin enters intestinal epithelial Caco-2 cells by fluid-phase endocytosis. *PLoS One, 9*(1), e84856.
Fenyvesi, F., Kiss, T., Fenyvesi, É., Szente, L., Veszelka, S., Deli, M. A., et al. (2011). Randomly methylated β-cyclodextrin derivatives enhance taxol permeability through human intestinal epithelial Caco-2 cell monolayer. *Journal of Pharmaceutical Sciences, 100*(11), 4734–4744.
Ferreira, L. G., & Andricopulo, A. D. (2016). Drug repositioning approaches to parasitic diseases: A medicinal chemistry perspective. *Drug Discovery Today, 21*(10), 1699–1710.
Figueroa-Guinez, R., Matos, M. J., Saleta, V. R., Lourdes, S., Eugenio, U., Borges, F., et al. (2015). The interest of antioxidants agents in parasitic diseases. The case study of coumarins. *Current Topics and Medicinal Chemistry, 15*(9).
Folch-Cano, C., Olea-Azar, C., Sobarzo-Sánchez, E., Alvarez-Lorenzo, C., Concheiro, A., Otero, F., et al. (2011). Inclusion complex of 4-hydroxycoumarin with cyclodextrins and its characterization in aqueous solution. *Journal of Solution Chemistry, 40*(11), 1835–1846.
Freitas, R. F., Prokopczyk, I. M., Zottis, A., Oliva, G., Andricopulo, A. D., Trevisan, M. T. S., et al. (2009). Discovery of novel *Trypanosoma cruzi* glyceraldehyde-3-phosphate dehydrogenase inhibitors. *Bioorganic & Medicinal Chemistry, 17*(6), 2476–2482.
Genes, C., Baquero, E., Echeverri, F., Maya, J. D., & Triana, O. (2011). Mitochondrial dysfunction in *Trypanosoma cruzi*: The role of Serratia marcescens prodigiosin in the alternative treatment of Chagas disease. *Parasit Vectors, 4*(66), 1–8.
Han, X.-J., Dong, Z.-Q., Fan, M.-M., Liu, Y., li, J.-H., Wang, Y.-F., et al. (2012). pH-induced shape-memory polymers. *Macromolecular Rapid Communications, 33*(12), 1055–1060.
Haug, A., Larsen, B., & Smidsrød, O. (1974). Uronic acid sequence in alginate from different sources. *Carbohydrate Research, 32*(2), 217–225.
Hoffman, A. S. (2002). Hydrogels for biomedical applications. *Advanced Drug Delivery Reviews, 54*(1), 3–12.
Hoshiyama, M., Kubo, K., Igarashi, T., & Sakurai, T. (2001). Complexation and proton dissociation behavior of 7-hydroxy-4-methylcoumarin and related compounds in the presence of β-cyclodextrin. *Journal of Photochemistry and Photobiology A: Chemistry, 138*(3), 227–233.
Izawa, H., Kawakami, K., Sumita, M., Tateyama, Y., Hill, J. P., & Ariga, K. (2013). [small beta]-Cyclodextrin-crosslinked alginate gel for patient-controlled drug delivery systems: Regulation of host-guest interactions with mechanical stimuli. *Journal of Materials Chemistry B, 1*(16), 2155–2161.
Job, P. (1928). Formation and stability of inorganic complexez in solution. *Annali di*

Chimica Applicata, 9, 113–203.
Kelly, B. J., & Brown, M. T. (2000). Variations in the alginate content and composition of Durvillaea antarctica and D. willana from southern New Zealand. *Journal of Applied Phycology, 12*(3), 317–324.
Kim, B., La Flamme, K., & Peppas Nicholas, A. (2003). Dynamic swelling behavior of pH-sensitive anionic hydrogels used for protein delivery. *Journal of Applied Polymer Science, 89*(6), 1606–1613.
Kobo, P. I., Ayo, J. O., Aluwong, T., Zezi, A. U., Maikai, V., & Ambali, S. F. (2014). Flavonoid mixture ameliorates increase in erythrocyte osmotic fragility and malondialdehyde concentration induced by Trypanosoma brucei brucei-infection in Wistar rats. *Research in Veterinary Science, 96*(1), 139–142.
Korsmeyer, R. W., Gurny, R., Doelker, E., Buri, P., & Peppas, N. A. (1983). Mechanisms of solute release from porous hydrophilic polymers. *International Journal of Pharmaceutics, 15*(1), 25–35.
Kurkov, S. V., & Loftsson, T. (2013). Cyclodextrins. *International Journal of Pharmaceutics, 453*(1), 167–180.
Leal, D., De Borggraeve, W., Encinas, M. V., Matsuhiro, B., & Müller, R. (2013). Preparation and characterization of hydrogels based on homopolymeric fractions of sodium alginate and PNIPAAm. *Carbohydrate Polymers, 92*(1), 157–166.
Leal, D., Matsuhiro, B., Rossi, M., & Caruso, F. (2008). FT-IR spectra of alginic acid block fractions in three species of brown seaweeds. *Carbohydrate Research, 343*(2), 308–316.
Lecca, D., Nevin, D. K., Mulas, G., Casu, M. A., Diana, A., Rossi, D., et al. (2015). Neuroprotective and anti-inflammatory properties of a novel non-thiazolidinedione PPAR gamma agonist *in vitro* and in MPTP-treated mice. *Neuroscience, 302*, 23–35.
Lee, K. Y., & Mooney, D. J. (2012). Alginate: Properties and biomedical applications. *Progress in Polymer Science, 37*(1), 106–126.
Leonardi, D., Bombardiere, M. E., & Salomon, C. J. (2013). Effects of benznidazole:cyclodextrin complexes on the drug bioavailability upon oral administration to rats. *International Journal of Biological Macromolecules, 62*(0), 543–548.
Li, D., Chen, L., Yi, X., Zhang, X., & Ye, N. (2010). Pyrolytic characteristics and kinetics of two brown algae and sodium alginate. *Bioresource Technology, 101*(18), 7131–7136.
Loftsson, T., Vogensen, S. B., Brewster, M. E., & Konráosdóttir, F. (2007). Effects of cyclodextrins on drug delivery through biological membranes. *Journal of Pharmaceutical Sciences, 96*(10), 2532–2546.
Louiz, S., Labiadh, H., & Abderrahim, R. (2015). Synthesis and spectroscopy studies of the inclusion complex of 3-amino-5-methyl pyrazole with beta-cyclodextrin. *Spectrochimica Acta Part A: Molecular and Biomolecular Spectroscopy, 134*, 276–282.
Lucas-Abellan, C., Fortea, I., Gabaldon, J. A., & Nunez-Delicado, E. (2008). Encapsulation of quercetin and myricetin in cyclodextrins at acidic pH. *Journal of Agricultural and Food Chemistry, 56*(1), 255–259.
Malaquias, L. F. B., Sá-Barreto, L. C. L., Freire, D. O., Silva, I. C. R., Karan, K., Durig, T., et al. (2018). Taste masking and rheology improvement of drug complexed with beta-cyclodextrin and hydroxypropyl-β-cyclodextrin by hot-melt extrusion. *Carbohydrate Polymers, 185*, 19–26.
Mansilla, A. O., Avila, M., & Cáceres, J. (2017). Reproductive biology of *Durvillaea antarctica* (Chamisso) Hariot in the sub-Antartic ecoregion of Magallanes (51–56°S). *Journal of Applied Phycology, 29*(5), 2567–2574.
Martínez-Gómez, F., Guerrero, J., Matsuhiro, B., & Pavez, J. (2017). *In vitro* release of metformin hydrochloride from sodium alginate/polyvinyl alcohol hydrogels. *Carbohydrate Polymers, 155*, 182–191.
Martínez-Gómez, F., Guerrero, J., Matsuhiro, B., & Pavez, J. (2018). Characterization of poly-D-mannuronate and poly-L-guluronate block fractions from sodium alginate and preparation of hydrogels with poly(vinylalcohol). *International Journal of Biological Macromolecules, 111*, 935–946.
Martínez-Gómez, F., Mansilla, A., Matsuhiro, B., Matulewicz, M. C., & Troncoso-Valenzuela, M. A. (2016). Chiroptical characterization of homopolymeric block fractions in alginates. *Carbohydrate Polymers, 146*, 90–101.
Matsuhiro, B., Torres, S. E., & Guerrero, J. (2007). Bloock structure in alginic acid from *Lessonia vadosa* (Laminariales, Phaeophyta). *Journal of the Chilean Chemical Society, 52*, 1095–1098.
Matsuhiro, B., Leal, D., & Mansilla, A. (2012). *Alginic acids from phaeophyta of Magellan Region (Chile). Alginates: Production, types and applications*. Nova Science Publishers, Inc.217–234.
Matsuhiro, B., Martínez-Gómez, F., & Mansilla, A. (2015). *Vibrational spectroscopy characterization of sodium alginate and its heteropolymeric and homopolymeric block fractions. Alginic acid: Chemical structure, uses and health benefits*. Future Medicine Ltd.89–103.
Méndez, F., Tala, F., Rautenberger, R., Ojeda, J., Rosenfeld, S., Rodríguez, J. P., et al. (2017). Morphological and physiological differences between two morphotypes of *Durvillaea antarctica* (Phaeophyceae) from the sub-Antarctic ecoregion of Magallanes, Chile. *Journal of Applied Phycology, 29*(5), 2557–2565.
Menezes, I. R., Lopes, J. C., Montanari, C. A., Oliva, G., Pavao, F., Castilho, M. S., et al. (2003). 3D QSAR studies on binding affinities of coumarin natural products for glycosomal GAPDH of *Trypanosoma cruzi*. *Journal of Computer-Aided Molecular Design, 17*(5-6), 277–290.
Menna-Barreto, R. F. S., Goncalves, R. L. S., Costa, E. M., Silva, R. S. F., Pinto, A. V., Oliveira, M. F., et al. (2009). The effects on *Trypanosoma cruz*i of novel synthetic naphthoquinones are mediated by mitochondrial dysfunction. *Free Radical Biology and Medicine, 47*(5), 644–653.
Miranda, N., Gerola, A. P., Novello, C. R., Ueda-Nakamura, T., de Oliveira Silva, S., Dias-Filho, B. P., et al. (2017). Pheophorbide a, a compound isolated from the leaves of Arrabidaea chica, induces photodynamic inactivation of *Trypanosoma cruzi*. *Photodiagnosis and Photodynamic Therapy, 19*, 256–265.
Miranda, N., Volpato, H., da Silva Rodrigues, J. H., Caetano, W., Ueda-Nakamura, T., de Oliveira Silva, S., et al. (2017). The photodynamic action of pheophorbide a induces cell death through oxidative stress in *Leishmania amazonensis*. *Journal of Photochemistry and Photobiology B: Biology, 174*, 342–354.
Mocanu, G., Mihai, D., LeCerf, D., Picton, L., & Moscovici, M. (2009). Cyclodextrin-anionic polysaccharide hydrogels: Synthesis, characterization, and interaction with some organic molecules (water pollutants, drugs, proteins). *Journal of Applied Polymer Science, 112*(3), 1175–1183.
Moncada-Basualto, M., Lapier, M., Maya, J. D., Matsuhiro, B., Olea-Azar, C. L., Delogu, G., et al. (2018). Evaluation of trypanocidal and antioxidant activities of a selected series of 3-amidocoumarins. *Medicinal Chemistry, 14*, 1–12.
Morais, C. A. S., Lemes Silva, B., Denadai, A. M. L., Fedoce Lopes, J., & De Sousa, F. B. (2017). Structural and thermodynamic investigation of pentoxifylline-cyclodextrin inclusion complex. *Chemical Physics Letters, 682*(16), 43–48.
Mosmann, T. (1983). Rapid colorimetric assay for cellular growth and survival: Application to proliferation and cytotoxicity assays. *Journal of Immunological Methods, 65*(1), 55–63.
Muñoz, A., Fonseca, A., Matos, M. J., Uriarte, E., Santana, L., Borges, F., et al. (2016). Evaluation of antioxidant and antitrypanosomal properties of a selected series of synthetic 3-carboxamidocoumarins. *ChemistrySelect, 1*(15), 4957–4964.
Nogueira, N. P., Saraiva, F. M. S., Oliveira, M. P., Mendonça, A. P. M., Inacio, J. D. F., Almeida-Amaral, E. E., et al. (2017). Heme modulates *Trypanosoma cruzi* bioenergetics inducing mitochondrial ROS production. *Free Radical Biology and Medicine, 108*, 183–191.
Nunes, M. C. P., Dones, W., Morillo, C. A., Encina, J. J., & Ribeiro, A. L. (2013). Chagas disease: An overview of clinical and epidemiological aspects. *Journal of the American College of Cardiology, 62*(9), 767–776.
Peppas, N. A., Bures, P., Leobandung, W., & Ichikawa, H. (2000). Hydrogels in pharmaceutical formulations. *European Journal of Pharmaceutics and Biopharmaceutics, 50*(1), 27–46.
Pérez-Molina, J. A., & Molina, I. (2018). Chagas disease. *The Lancet, 391*(10115), 82–94.
Pinho, E., Grootveld, M., Soares, G., & Henriques, M. (2014). Cyclodextrins as encapsulation agents for plant bioactive compounds. *Carbohydrate Polymers, 101*(0), 121–135.
Rekharsky, M. V., Mayhew, M. P., Goldberg, R. N., Ross, P. D., Yamashoji, Y., & Inoue, Y. (1997). Thermodynamic and nuclear magnetic resonance study of the reactions of α- and β-cyclodextrin with acids, aliphatic amines, and cyclic alcohols. *The Journal of Physical Chemistry B, 101*(1), 87–100.
Ren, B., Gao, H., Cao, Y., & Jia, L. (2015). In silico understanding of the cyclodextrin-phenanthrene hybrid assemblies in both aqueous medium and bacterial membranes. *Journal of Hazardous Materials, 285*, 148–156.
Reszka, K., Cruz, F. S., & Docampo, R. (1986). Photosensitization by the trypanocidal agent crystal violet. Type I versus type II reactions. *Chemico-Biological Interactions, 58*, 161–172.
Réti-Nagy, K., Malanga, M., Fenyvesi, É., Szente, L., Vámosi, G., Váradi, J., et al. (2015). Endocytosis of fluorescent cyclodextrins by intestinal Caco-2 cells and its role in paclitaxel drug delivery. *International Journal of Pharmaceutics, 496*(2), 509–517.
Roy, A., Saha, S., & Roy, M. N. (2016). Study to explore host-guest inclusion complexes of cyclodextrins with biologically active molecules in aqueous environment. *Fluid Phase Equilibria, 425*, 252–258.
Sierpe, R., Noyong, M., Simon, U., Aguayo, D., Huerta, J., Kogan, M. J., et al. (2017). Construction of 6-thioguanine and 6-mercaptopurine carriers based on βcyclodextrins and gold nanoparticles. *Carbohydrate Polymers, 177*, 22–31.
Soares-Sobrinho, J. L., Santos, F. L. A., Lyra, M. A. M., Alves, L. D. S., Rolim, L. A., Lima, A. A. N., et al. (2012). Benznidazole drug delivery by binary and multicomponent inclusion complexes using cyclodextrins and polymers. *Carbohydrate Polymers, 89*(2), 323–330.
Svanem, B. I., Skjak-Braek, G., Ertesvag, H., & Valla, S. (1999). Cloning and expression of three new Aazotobacter vinelandii genes closely related to a previously described gene family encoding mannuronan C-5-epimerases. *Journal of Bacteriology, 181*(1), 68–77.
Tablet, C., Matei, I., & Hillebrand, M. (2012). The determination of the stoichiometry of cyclodextrin inclusion complexes by spectral methods: Possibilities and limitations. *INTECH, 3*, 48–76.
Tang, W., & Ng, S.-C. (2008). Facile synthesis of mono-6-amino-6-deoxy-[alpha]-, [beta]-, [gamma]-cyclodextrin hydrochlorides for molecular recognition, chiral separation and drug delivery. *Nature Protocols, 3*(4), 691–697.
Venegas, M., Matsuhiro, B., & Edding, M. E. (1993). Alginate composition of *Lessonia trabeculata* (Phaeophyta: Laminariales) growing in exposed and sheltered habitats. *Botanica Marina, 36*, 47.
Vieites, M., Otero, L., Santos, D., Toloza, J., Figueroa, R., Norambuena, E., et al. (2008). Platinum(II) metal complexes as potential anti-*Trypanosoma cruzi* agents. *Journal of Inorganic Biochemistry, 102*(5), 1033–1043.
Wahid, F., Wang, H.-S., Zhong, C., & Chu, L.-Q. (2017). Facile fabrication of moldable antibacterial carboxymethyl chitosan supramolecular hydrogels cross-linked by metal ions complexation. *Carbohydrate Polymers, 165*(Suppl. C), 455–461.
Wu, W., Zhang, Z., Xiong, T., Zhao, W., Jiang, R., Chen, H., et al. (2017). Calcium ion coordinated dexamethasone supramolecular hydrogel as therapeutic alternative for control of non-infectious uveitis. *Acta Biomaterialia, 61*(Suppl. C), 157–168.
Yang, C., Liu, L., Mu, T.-W., & Guo, Q.-X. (2001). Improved accuracy and efficiency in the determination of association constants with the spectrophotometric method. *Journal of Inclusion Phenomena and Macrocyclic Chemistry, 39*(1), 97–101.
Yang, L., Li, M., Sun, Y., & Zhang, L. (2018). A cell-penetrating peptide conjugated carboxymethyl-β-cyclodextrin to improve intestinal absorption of insulin. *International Journal of Biological Macromolecules, 111*, 685–695.